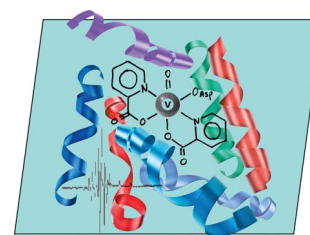


DOI:10.1002/ejic.201402408

## Vanadium Complexes as Prospective Therapeutics: Structural Characterization of a V<sup>IV</sup> Lysozyme Adduct

Marino F. A. Santos,<sup>[a]</sup> Isabel Correia,<sup>[b]</sup> Ana R. Oliveira,<sup>[a]</sup>  
Eugenio Garribba,<sup>[c]</sup> João Costa Pessoa,\*<sup>[b]</sup> and  
Teresa Santos-Silva\*<sup>[a]</sup>



COVER PICTURE

**Keywords:** Vanadium / Protein adducts / Medicinal chemistry / EPR spectroscopy / Density functional calculations

The biological activity of vanadium complexes, namely, as insulin enhancers, is well known. We report a combined X-ray crystallography, electron paramagnetic resonance, and density functional theory study of the interaction of vanadium picolinate complexes with hen egg white lysozyme

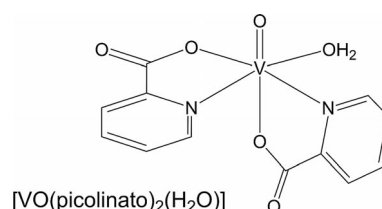
(HEWL). We show that the V<sup>IV</sup>O(pic)<sub>2</sub> complex covalently binds to the COO<sup>-</sup> group of the side chain of Asp52 of HEWL. The long V<sup>IV</sup>=O bond obtained in the X-ray study is explained to be due to reduction of V<sup>IV</sup> to V<sup>III</sup> during exposure of the crystals to the intense X-ray beam.

### Introduction

Vanadium is a transition metal that has been implicated in the last decades in the fields of medicine and pharmacology owing to its physiological role as insulin-enhancer,<sup>[1]</sup> anticancer,<sup>[2]</sup> and antiparasitic agent.<sup>[3]</sup> Moreover, vanadium has been found to take relevant roles in some nitrogenases and haloperoxidases, and a few single-crystal X-ray structures are available for several of the vanadium haloperoxidase enzymes.<sup>[4]</sup>

To have a physiological role, vanadium needs to be first transported in the blood and then taken up by the cells. This process is most likely conducted by plasma proteins such as human serum transferrin (hTF) and human serum albumin.<sup>[5]</sup> It is known that hTF is the prevailing vehicle for vanadium transport. In normal serum, only about 30% of the total binding sites are occupied by iron;<sup>[6]</sup> this means that there are available sites for other metal ions, without the need to replace tightly bound Fe<sup>III</sup>.<sup>[5a,5c,7]</sup> It was demonstrated that if vanadium is administered in the form of a

complex, for example, V<sup>IV</sup>O(carrier)<sub>2</sub>, in which carrier is an organic ligand, often the doses needed to achieve the same therapeutic effect are significantly lower. Among the several VO complexes exhibiting insulin-enhancing properties, V<sup>IV</sup>O(maltolato)<sub>2</sub> and derivatives have been extensively studied from the chemical and pharmacological points of view<sup>[1b,8]</sup> as has V<sup>IV</sup>O(picolinato)<sub>2</sub><sup>[9]</sup> and V<sup>V</sup>-dipicolinato compounds.<sup>[10]</sup> In particular [VO(picolinato)<sub>2</sub>(H<sub>2</sub>O)] (Scheme 1) was shown to be a strong inhibitor of fatty acid mobilization and effective in the treatment of rats affected by diabetes induced with streptozotocin.<sup>[9,10]</sup> If V is introduced in the blood stream in the form of a V<sup>IV</sup>O(carrier)<sub>2</sub> complex, these carrier ligands may also participate in the transport of vanadium in blood.<sup>[5]</sup> The mode of action of this metal is not well understood and is still the subject of much debate.<sup>[1b,8,11]</sup> Particularly, the interaction of these complexes with serum, membrane, or cytosolic proteins is an important aspect, as it controls their ADME (absorption, distribution, metabolism, and excretion) properties and efficacy.



Scheme 1. Structural formula of a vanadium complex formed by the picolinato<sup>-</sup> (pic<sup>-</sup>) ligand.

Hen egg white lysozyme (HEWL) has been used as a model protein for X-ray crystallography, similar to what has been done for other metal-based drugs.<sup>[12]</sup> In this work, we studied the interaction of V<sup>IV</sup>O(pic)<sub>2</sub> (pic = picolinato<sup>-</sup>

[a] UCIBIO@REQUIMTE, Departamento de Química, Faculdade de Ciências e Tecnologia, Universidade Nova de Lisboa, 2829-516 Caparica, Portugal  
E-mail: tsss@fct.unl.pt  
http://sites.fct.unl.pt/xtal

[b] Centro de Química Estrutural, Instituto Superior Técnico, Universidade Lisboa, Av. Rovisco Pais, 1049-001 Lisboa, Portugal  
E-mail: joao.pessoa@ist.utl.pt  
http://cqe.ist.utl.pt/

[c] Dipartimento di Chimica e Farmacia and Centro Interdisciplinare per lo Sviluppo della Ricerca Biotecnologica e per lo Studio della Biodiversità della Sardegna, Università di Sassari, Via Vienna 2, 07100 Sassari, Italia

Supporting information for this article is available on the WWW under <http://dx.doi.org/10.1002/ejic.201402408>.

anion) with HEWL and present the first X-ray structure of a V<sup>IV</sup>O compound covalently bound to a protein, which can be relevant to understand the pharmacological action of this and other prospective drugs.

## Results and Discussion

HEWL crystals prepared upon soaking with a solution of V<sup>IV</sup>OSO<sub>4</sub>/picolinic acid (molar ratio of 1:3) diffracted beyond a resolution of 1.28 Å (see the Supporting Information; PDB code 4c3w). Analysis of the electron density map of the HEWL structure revealed a strong peak at the active site of the enzyme, close to the Asp52 residue, at which a V<sup>IV</sup>O(pic)<sub>2</sub> moiety could be modeled with an occupancy of 0.65. An anomalous electron density map was also calculated and a strong peak for V was clearly observed (Figure S1, Supporting Information).

Vanadium adopts a distorted octahedral geometry covalently bound to Asp52, with a bidentate coordination to two pic<sup>-</sup> anions and an O<sub>oxido</sub> atom (Figure 1). The V=O bonds typically vary between 1.57 and 1.65 Å.<sup>[14]</sup> In the present case, the V<sup>IV</sup>=O bond length determined by X-ray analysis is quite long (1.82 Å), whereas that of V<sup>IV</sup>-O (Asp52) is relatively short (1.89 Å). Asn46 is found close to the complex, and it interacts with the O<sub>oxido</sub> atom through a hydrogen bond. This interaction could be responsible for the anomalous distance observed. However, X-ray-induced reduction owing to the very intense beam used for data collection is a more plausible explanation. Partial reduction of the metal from the +4 oxidation state to the +3 oxidation state, which occurs during radiation exposure, may explain the large distance between V and O<sub>oxido</sub>. This type of phenomenon has been reported for metalloenzymes,<sup>[15]</sup> and in the present case it would correspond to a progressive change during radiation exposure from a V<sup>IV</sup>=O bond to a V<sup>III</sup>-O bond with concomitant elongation of the bond length. To test this hypothesis, model refinement was conducted by using different slices of the collected data for further comparison with the final model.

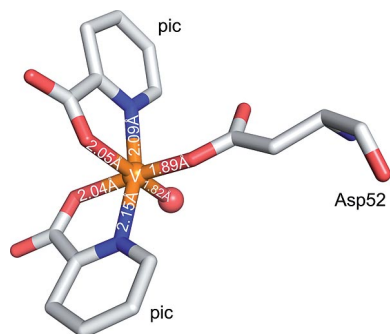


Figure 1. Structural representation of the V<sup>IV</sup>O(pic)<sub>2</sub>-Asp52 fragment of the HEWL-V<sup>IV</sup>O(pic)<sub>2</sub> adduct. Bond lengths between V and the donor atoms are indicated (see also text). Picture was prepared by using Pymol.<sup>[13]</sup>

Table 1 shows the measured distances between V and all donor atoms: for the complete data set, the first 350 images,

the first 500 images, and also the last 500 images collected. Even though the obtained completeness for the studied subsets is not ideal, it is clear that pronounced changes occur during data collection, specially for the V=O bond. Hence, whereas in the early stages of data collection (initial 35% of the dataset used) the distance between the metal and the O<sub>oxido</sub> ligand is 1.76 Å, this value increases by the end of the data collection (final 50% of the data used) up to 1.85 Å. These differences suggest that V is reduced during data collection. Large distances previously obtained for V<sup>V</sup>=O bonds in other vanadium-protein studies<sup>[16]</sup> may have also resulted from reduction induced by radiation. Regarding the V-O(pic) bond lengths determined, these are very similar (2.04 and 2.05 Å) although the one involving the O atom *trans* to the O<sub>oxido</sub> ligand is rather short.<sup>[14]</sup>

Table 1. Distance between V and the coordinating ligands for the complete data set, the first 350 images, the first 500 images, and the last 500 images collected.

Bond	Distance [Å]			
	Images 1–1000	Images 1–350	Images 1–500	Images 501–1000
V=O	1.82	1.76	1.78	1.85
V-Asp52	1.89	1.91	1.90	1.93
V-N (pic1)	2.09	2.13	2.11	2.10
V-O (pic1)	2.05	2.05	2.03	2.07
V-N (pic2)	2.15	2.16	2.19	2.11
V-O (pic2)	2.04	2.02	2.01	2.04

To confirm the oxidation state of V, electron paramagnetic resonance (EPR) experiments of the HEWL-V adduct crystals were undertaken. The spectra obtained at room temperature with a suspension of the crystals in buffer (Figure S2) and for the same suspension frozen at 77 K (Figure 2) exhibited a hyperfine pattern; this confirms the presence of a monomeric V<sup>IV</sup>O-bound species with a d<sub>xy</sub><sup>1</sup> ground-state configuration, and the following spin Hamiltonian parameters (the *g* factors and the hyperfine structure constants, *A*) were obtained:<sup>[17]</sup> (1) for the spectrum at 77 K:  $g_x = 1.985$ ,  $g_y = 1.985$ ,  $g_z = 1.951$ ,  $A_x = -57.6 \times 10^{-4} \text{ cm}^{-1}$ ,  $A_y = -57.8 \times 10^{-4} \text{ cm}^{-1}$ ,  $A_z =$

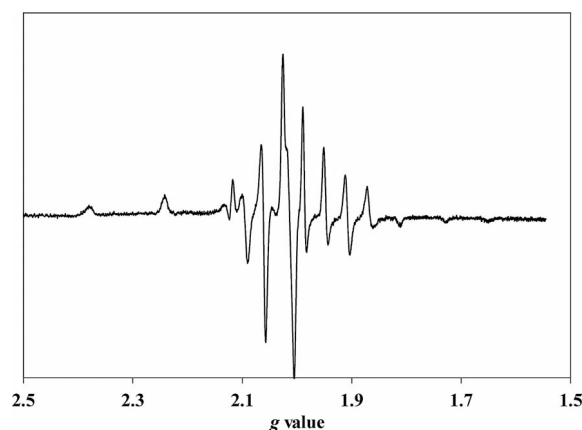


Figure 2. First derivative X-band EPR spectrum of a suspension in buffer of pH ≈ 4.5, frozen at 77 K, of the HEWL-V<sup>IV</sup>O(pic)<sub>2</sub> adduct crystals.

$-164.5 \times 10^{-4} \text{ cm}^{-1}$ ; (2) for the spectrum measured at room temperature:  $g_{\text{iso}} = 1.975$  and  $A_{\text{iso}} = -92.4 \times 10^{-4} \text{ cm}^{-1}$ . The parameters reported for  $\text{V}^{\text{IV}}\text{O}(\text{pic})_2(\text{H}_2\text{O})$  (Scheme 1) are:  $g_z = 1.945$ ,  $A_z = -165 \times 10^{-4} \text{ cm}^{-1}$ .<sup>[18]</sup>

The  $^{51}\text{V}$  hyperfine coupling tensor **A** was calculated by DFT methods (see the Supporting Information), and the results are shown in Table 2. From the X-ray structure of the HEWL– $\text{V}^{\text{IV}}\text{O}(\text{pic})_2$  adduct crystals, only the residues at less than 8 Å from V were considered. On the resulting structure (V–HEWL in Table 2), the  $^{51}\text{V}$  ( $A_{\text{iso}}$ ,  $A_x$ ,  $A_y$ , and  $A_z$ ) hyperfine coupling constants were calculated. The protonation state of Asp52 (V–HEWL<sup>H</sup>, Table 2) and the effect of the  $\text{V}^{\text{IV}}=\text{O}$  bond length on the  $^{51}\text{V}$  **A** tensor (V<sup>VO</sup>–HEWL, Table 2) were also studied by DFT methods. The value of  $A_z^{\text{calcd.}}$  calculated by using the coordinates of the X-ray structure (V–HEWL) is very far from the experimental one, which is due to the large distance found for the V=O bond relative to usual bond lengths (1.82 vs. 1.57–1.65 Å).<sup>[14]</sup> If this was indeed the case, the V–HEWL adduct, as determined by the X-ray study, would resemble a non-oxido  $\text{V}^{\text{IV}}$  complex (with a V–O bond), for which low  $A_z$  values are expected.<sup>[19]</sup> The spin Hamiltonian parameters with the same coordinates but with the carboxylate side group of Asp52 protonated (V–HEWL<sup>H</sup>) were also calculated but did not bring much improvement in the prediction of  $A_z$ , as only a slight increase in  $|A_z^{\text{calcd.}}|$  was achieved.

Table 2. Calculated and experimental parameters for the HEWL– $\text{V}^{\text{IV}}\text{O}(\text{pic})_2$  adduct and related structures.<sup>[a]</sup>

	$A_{\text{iso}}^{\text{calcd.}}$	$A_x^{\text{calcd.}}$	$A_y^{\text{calcd.}}$	$A_z^{\text{calcd.}}$	$A_z^{\text{exp.}}$	Dev. [%] <sup>[b]</sup>
V–HEWL	–84.5	–48.7	–56.8	–148.1	–164.5	–10.0
V–HEWL <sup>H</sup>	–86.9	–50.8	–58.5	–150.6	–164.5	–8.4
V <sup>VO</sup> –HEWL	–93.6	–58.2	–61.9	–160.7	–164.5	–2.3
$\text{V}^{\text{IV}}\text{O}(\text{pic})_2\text{-(H}_2\text{O)}$ <sup>[18]</sup>	–96.5	–62.0	–64.1	–163.5 <sup>[21]</sup>	–165.0 <sup>[21]</sup>	–0.9

[a] All values measured in  $10^{-4} \text{ cm}^{-1}$ . [b] The % deviation of  $|A_z^{\text{calcd.}}|$  from  $|A_z^{\text{exp.}}|$ , expressed as  $100 \times [(|A_z^{\text{calcd.}}| - |A_z^{\text{exp.}}|)/|A_z^{\text{exp.}}|]$ .

Given that the critical point was the  $\text{V}^{\text{IV}}=\text{O}$  distance (1.82 Å, see Figure 1), an optimization of the position of  $\text{O}_{\text{oxido}}$  was performed by freezing the positions of all other atoms with the COO group of Asp52 in the deprotonated form; a distance of 1.601 Å for V=O was obtained. The calculation of  $^{51}\text{V}$   $A_z$  on this structure (V<sup>VO</sup>–HEWL, Table 2) gave good results: a deviation of –2.3% was observed, in agreement with the values reported for similar simulations.<sup>[20]</sup> The value for  $A_z$  of  $-160.7 \times 10^{-4} \text{ cm}^{-1}$  for V<sup>VO</sup>–HEWL also agrees with that calculated for *cis*- $[\text{V}^{\text{IV}}\text{O}(\text{pic})_2(\text{H}_2\text{O})]$  ( $-163.5 \times 10^{-4} \text{ cm}^{-1}$ ),<sup>[21]</sup> and the lower value is compatible with the replacement of a water molecule with a COO donor.<sup>[22]</sup> Moreover, the lower value of  $|A_x^{\text{calcd.}} - A_y^{\text{calcd.}}|$  obtained for V<sup>VO</sup>–HEWL relative to that obtained for V–HEWL or V–HEWL<sup>H</sup> is in very good agreement with the experimental EPR spectrum (Figure 2). In conclusion, these results indicate that in the crystal the  $\text{V}^{\text{IV}}=\text{O}$  bond of the V–HEWL adduct has its usual length. The long V=O bond obtained from the X-ray data is thus due to partial reduction induced by the intense X-ray radia-

tion used during the collection of the X-ray data, as already discussed.

To further confirm that the  $\text{V}^{\text{IV}}$  species responsible for the EPR signal is the bound complex and not free  $\text{V}^{\text{IV}}\text{O}(\text{pic})_2(\text{H}_2\text{O})$ , several days after the measurement of the spectrum of HEWL– $\text{V}^{\text{IV}}\text{O}(\text{pic})_2$  shown in Figure S2 (always keeping the samples at  $\approx 6^\circ\text{C}$ ), the spectrum were remeasured before and after dilution (1:3) with harvesting buffer (pH  $\approx 4.5$ ) of the suspension of the HEWL–V adduct crystals. The intensity of all EPR spectra was roughly the same; this indicates that the EPR signal is due to protein bound  $\text{V}^{\text{IV}}\text{O}(\text{pic})_2\text{–Asp52}$  and that this complex species, if bound to the protein in the crystals, is quite stable to hydrolysis and to oxidation. In fact, in the absence of any interaction with HEWL, the oxidation of  $\text{V}^{\text{IV}}\text{O}(\text{pic})_2(\text{H}_2\text{O})$  would be relatively fast at this pH.<sup>[14,18]</sup> Thus, EPR definitely confirms the presence of  $\text{V}^{\text{IV}}$  in the  $\text{V}^{\text{IV}}\text{O}(\text{pic})_2\text{–Asp52}$  adduct crystals, with a  $\text{V}^{\text{IV}}=\text{O}$  bond length close to 1.60 Å, as also predicted by DFT simulations.

Several experiments were also done by circular dichroism (CD) and EPR spectroscopy with buffered acetate solutions at pH 4.5. Figure 3 shows the obtained CD spectra. As the lysozyme does not absorb in the 400–1000 nm range, its CD spectrum corresponds to the baseline; thus, the  $\Delta\epsilon$  values measured with a solution containing HEWL and  $\text{V}^{\text{IV}}\text{O}(\text{pic})_2(\text{H}_2\text{O})$  correspond to a very weakly induced CD spectrum in which the d–d bands of  $\text{V}^{\text{IV}}\text{O}$  are clearly seen owing to binding of  $\text{V}^{\text{IV}}$  to the chiral donor atoms of the lysozyme. The pattern of the CD spectrum measured is similar to that measured for the monodentate coordination of the  $\text{COO}^-$  group of the amino acids to  $\text{V}^{\text{IV}}\text{O}$ ,<sup>[23]</sup> and the very low  $\Delta\epsilon$  values obtained are compatible with the coordination of an amino acid side group such as an O carboxylate. With solutions containing  $\text{V}^{\text{IV}}\text{OSO}_4$  and HEWL, no CD bands were detected in the 400–1000 nm range.

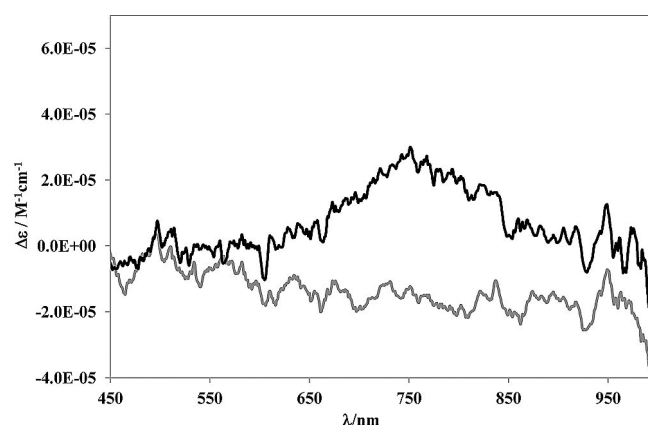


Figure 3. CD spectra measured in the visible region for solutions containing HEWL (0.7 mM, grey line) and HEWL/ $\text{V}^{\text{IV}}\text{OSO}_4/\text{pic}$  (0.7:0.7:1.5 mM, black line) in acetate buffer (0.1 M, pH 4.5), with an optical path length of 4 cm.

The EPR spectrum measured at 77 K with the solution of HEWL/ $\text{V}^{\text{IV}}\text{OSO}_4/\text{pic}$  used to record the CD spectrum of Figure 3 is very similar to that measured with the suspen-

sion of HEWL–V<sup>IV</sup>O(pic)<sub>2</sub> crystals, but it differs from the spectrum measured with the frozen solution of HEWL and V<sup>IV</sup>OSO<sub>4</sub> in acetate buffer at pH 4.5, for which the following spin Hamiltonian parameters were obtained:  $g_x, g_y = 1.982$ ,  $g_z = 1.943$ ,  $A_x, A_y = -64.7 \times 10^{-4} \text{ cm}^{-1}$ ,  $A_z = -175.9 \times 10^{-4} \text{ cm}^{-1}$ . These parameters suggest monodentate equatorial coordination of a COO<sup>-</sup> group of the protein to V<sup>IV</sup>O.

## Conclusion

In summary, scientists have dedicated much attention to V complexes owing to their biological activity, namely, as insulin enhancers. To further understand its transport in blood serum and its interactions with membrane or cytosolic proteins, the interaction of V<sup>IV</sup>O(pic)<sub>2</sub> with HEWL was studied by X-ray crystallography. Our results showed that the V<sup>IV</sup> ion of V<sup>IV</sup>O(pic)<sub>2</sub> can covalently bind to the COO<sup>-</sup> group of the Asp52 residue of HEWL by substituting the equatorial water molecule; this is the first example of V<sup>IV</sup>–protein binding confirmed by single-crystal X-ray diffraction. For the HEWL–V<sup>IV</sup>O(pic)<sub>2</sub> adduct, a relatively strong EPR signal was observed, and this confirmed the presence of V<sup>IV</sup>O species; DFT results allowed the binding of the carboxylate of the Asp52 residue of HEWL to the V<sup>IV</sup>O(pic)<sub>2</sub> moiety to be confirmed and allowed for the prediction that the V<sup>IV</sup>=O bond is in fact  $\approx 1.60 \text{ \AA}$  in the soaked crystals. However, in the refined crystallographic structure a relatively long bond was found between the metal and the O<sub>oxido</sub> donor (1.82 Å). As explained above, the reduction of V<sup>IV</sup> to V<sup>III</sup> during the beam exposure was corroborated by analysis of subsets of the diffraction images. This is a relevant finding, as similar reduction might explain anomalous structural data previously reported in V<sup>V</sup>-containing proteins.

V<sup>IV</sup>O carrier–protein adducts might form with transferrin, albumin,<sup>[5]</sup> or other proteins such as membrane or cytosolic proteins. We proved herein that V<sup>IV</sup>O carriers can bind strongly to proteins, as observed for HEWL, but more data is required to better understand the interaction of V<sup>IV</sup>O carrier compounds with serum proteins, particularly if this may promote the uptake of vanadium into cells. Elucidation of these processes is relevant for the development of complexes as putative therapeutic agents.

**Supporting Information** (see footnote on the first page of this article): Additional data for the HEWL–V adduct (X-ray crystallography and EPR) and DFT calculations.

## Acknowledgments

The authors would like to thank Fundação para a Ciência e Tecnologia (FCT) for funding [program Ciência 2007, 2008 and Investigador FCT; grants SFRH/BD/77894/2011 (to M. F. A. S.), PEst-C/EQB/LA0006/2013, and PEst-OE/QUI/UI0100/2013]. The research leading to these results has received funding from the European Community's Seventh Framework Programme (FP7/2007–2013) under BioStruct-X. The authors also acknowledge the

ESRF for provision of synchrotron radiation facilities (beamline ID29).

- [1] a) K. H. Thompson, C. Orvig, *J. Chem. Soc., Dalton Trans.* **2000**, 2885–2892; b) K. H. Thompson, J. Lichter, C. LeBel, M. C. Scaife, J. H. McNeill, C. Orvig, *J. Inorg. Biochem.* **2009**, *103*, 554–558.
- [2] A. M. Evangelou, *Crit. Rev. Oncol. Hematol.* **2002**, *42*, 249–265.
- [3] D. Gambino, *Coord. Chem. Rev.* **2011**, *255*, 2193–2203.
- [4] D. Rehder, *Bioinorganic Vanadium Chemistry*, John Wiley & Sons, New York, **2008**.
- [5] a) T. Kiss, T. Jakusch, D. Hollender, Á. Dörnyei, É. A. Enyedy, J. C. Pessoa, H. Sakurai, A. Sanz-Medel, *Coord. Chem. Rev.* **2008**, *252*, 1153–1162; b) G. R. Willsky, L.-H. Chi, M. Godzala Iii, P. J. Kostyniak, J. J. Smee, A. M. Trujillo, J. A. Alfano, W. Ding, Z. Hu, D. C. Crans, *Coord. Chem. Rev.* **2011**, *255*, 2258–2269; c) D. Sanna, G. Micera, E. Garribba, *Inorg. Chem.* **2010**, *49*, 174–187; d) T. Jakusch, D. Hollender, E. A. Enyedy, C. S. Gonzalez, M. Montes-Bayon, A. Sanz-Medel, J. C. Pessoa, I. Tomaz, T. Kiss, *Dalton Trans.* **2009**, 2428–2437; e) D. Sanna, L. Biro, P. Buglyo, G. Micera, E. Garribba, *Metallomics* **2012**, *4*, 33–36.
- [6] a) R. W. Evans, X. Kong, R. C. Hider, *Biochim. Biophys. Acta Gen. Subj.* **2012**, *1820*, 282–290; b) J. Williams, K. Moreton, *Biochem. J.* **1980**, *185*, 483–488.
- [7] a) H. Sun, H. Li, P. J. Sadler, *Chem. Rev.* **1999**, *99*, 2817–2842; b) T. Kiss, E. Kiss, E. Garribba, H. Sakurai, *J. Inorg. Biochem.* **2000**, *80*, 65–73; c) S. Mehtab, G. Gonçalves, S. Roy, A. I. Tomaz, T. Santos-Silva, M. F. A. Santos, M. J. Romão, T. Jakusch, T. Kiss, J. C. Pessoa, *J. Inorg. Biochem.* **2013**, *121*, 187–195.
- [8] P. W. Winter, A. Al-Qatati, A. L. Wolf-Ringwall, S. Schoeberl, P. B. Chatterjee, B. G. Barisas, D. A. Roess, D. C. Crans, *Dalton Trans.* **2012**, *41*, 6419–6430.
- [9] H. Sakurai, Y. Kojima, Y. Yoshikawa, K. Kawabe, H. Yasui, *Coord. Chem. Rev.* **2002**, *226*, 187–198.
- [10] D. C. Crans, L. Yang, T. Jakusch, T. Kiss, *Inorg. Chem.* **2000**, *39*, 4409–4416.
- [11] a) D. Rehder, *Future Med. Chem.* **2012**, *4*, 1823–1837; b) J. C. Pessoa, I. Tomaz, *Curr. Med. Chem.* **2010**, *17*, 3701–3738.
- [12] a) A. Casini, G. Mastrobuoni, C. Temperini, C. Gabbiani, S. Francese, G. Moneti, C. T. Supuran, A. Scozzafava, L. Messeri, *Chem. Commun.* **2007**, 156–158; b) M. Razavet, V. Artero, C. Cavazza, Y. Oudart, C. Lebrun, J. C. Fontecilla-Camps, M. Fontecave, *Chem. Commun.* **2007**, 2805–2807; c) S. L. Binkley, C. J. Ziegler, R. S. Herrick, R. S. Rowlett, *Chem. Commun.* **2010**, *46*, 1203–1205; d) T. Santos-Silva, A. Mukhopadhyay, J. D. Seixas, G. J. L. Bernardes, C. C. Romão, M. J. Romão, *J. Am. Chem. Soc.* **2011**, *133*, 1192–1195; e) M. F. A. Santos, J. D. Seixas, A. C. Coelho, A. Mukhopadhyay, P. M. Reis, M. J. Romão, C. C. Romão, T. Santos-Silva, *J. Inorg. Biochem.* **2012**, *117*, 285–291.
- [13] W. L. DeLano, *Pymol*, Delano Scientific, San Carlos, CA, **2002**; www.pymol.org.
- [14] L. F. V. Boas, J. C. Pessoa, *Comprehensive Coordination Chemistry*, vol. 3 (Eds.: R. D. G. G. Wilkinson, J. A. McCleverty), Pergamon Press, Oxford, UK, **1987**, p. 454–569.
- [15] a) G. I. Berglund, G. H. Carlsson, A. T. Smith, H. Szoke, A. Henriksen, J. Hajdu, *Nature* **2002**, *417*, 463–468; b) J. Wuerger, J.-W. Lee, Y.-I. Yim, H.-S. Yim, S.-O. Kang, K. D. Carugo, *Proc. Natl. Acad. Sci. USA* **2004**, *101*, 8569–8574.
- [16] A. Messerschmidt, L. Prade, R. Wever, *Biol. Chem.* **1997**, *378*, 309–316.
- [17] A. Rockenbauer, L. Korecz, *Appl. Magn. Reson.* **1996**, *10*, 29–43.
- [18] E. Kiss, E. Garribba, G. Micera, T. Kiss, H. Sakurai, *J. Inorg. Biochem.* **2000**, *78*, 97–108.
- [19] a) B. Morgenstern, B. Kutzky, C. Neis, S. Stucky, K. Hegetschweiler, E. Garribba, G. Micera, *Inorg. Chem.* **2007**, *46*,

- 3903–3915; b) D. Sanna, K. Várnagy, N. Lihi, G. Micera, E. Garribba, *Inorg. Chem.* **2013**, *52*, 8202–8213.
- [20] a) G. Micera, E. Garribba, *Dalton Trans.* **2009**, 1914–1918; b) G. Micera, E. Garribba, *J. Comput. Chem.* **2011**, *32*, 2822–2835; c) S. Gorelsky, G. Micera, E. Garribba, *Chem. Eur. J.* **2010**, *16*, 8167–8180.
- [21] E. Lodyga-Chruscinska, G. Micera, E. Garribba, *Inorg. Chem.* **2011**, *50*, 883–899.
- [22] T. S. Smith II, R. LoBrutto, V. L. Pecoraro, *Coord. Chem. Rev.* **2002**, *228*, 1–18.
- [23] a) J. C. Pessoa, L. F. V. Boas, R. D. Gillard, R. J. Lancashire, *Polyhedron* **1988**, *7*, 1245–1262; b) J. C. Pessoa, R. L. Marques, L. F. V. Boas, R. D. Gillard, *Polyhedron* **1990**, *9*, 81–98.

Received: May 8, 2014

Published Online: June 4, 2014